Vol. 25, No. 1(2026) Alim26706

Revista Mexicana de Ingeniería Química

Influence of extrusion conditions and microwave expansion on the mechanical, physical, and structural properties of third-generation snacks made with alternative flours using a twin-screw extruder

Influencia de las condiciones de extrusión y de la expansión por microondas en las propiedades mecánicas, físicas y estructurales de botanas de tercera generación elaboradas con harinas alternativas mediante una extrusor de doble tornillo

D. Neder-Suárez[1], D. Lardizábal-Gutiérrez[2], J. de J. Zazueta-Morales[3], J.A. Vázquez-Rodríguez[4], C.A. Amaya-Guerra[5], C.O. Meléndez-Pizarro[1], M. Márquez-Rivera[1], L.R. Hernández-Ochoa[1], A. Quintero-Ramos[1]*

[1]Facultad de Ciencias Químicas, Universidad Autónoma de Chihuahua, Circuito Universitario s/n Campus Universitario 2, Chihuahua, Chihuahua 31125, México [2]Centro de Investigación en Materiales Avanzados, S.C. Avenida Miguel de Cervantes 120, Complejo Industrial Chihuahua, Chihuahua 31109, México. [3]Facultad de Ciencias Químico Biológicas, Universidad Autónoma de Sinaloa, Ciudad Universitaria, Culiacán, Sinaloa 80000, México. Universidad Autónoma de Nuevo León, [4]Facultad de Salud Pública y Nutrición, Dr. Eduardo Aguirre Pequeño 905, Mitras Centro, Monterrey, N.L. 64460, México. [5]Facultad de Ciencias Biológicas, U. Autónoma de Nuevo León, Dr. E. Aguirre Pequeño 905, Monterrey 64460, México.

Received: October 30, 2025; Accepted: January 15, 2026

Abstract

This study evaluated the effects of extrusion and microwave expansion on the structural properties of mixtures of rice, white beans, and powdered red pitaya for the production of third-generation snacks. Mixtures with a moisture content of 27% were subjected to extrusion cooking at different temperatures (ETs; 90, 103, 116, and 129°C) and screw speeds (SSs; 75, 100, and 125 rpm) and subsequently subjected to microwave expansion. During extrusion, residence time (RDT) and specific mechanical energy were evaluated, also degree of starch gelatinization (DSG), *in vitro* starch digestibility (SD), storage modulus (G'), loss modulus (G"), apparent viscosity (η), expansion ratio (ER), flexural modulus (M_f), moment of inertia (M_I), enthalpy of gelatinization (ΔH), and microstructural properties were evaluated in the extruded products. After extrusion, RDT, DSG, SD, η, G', G", M_f, M_I, and ER increased, whereas ΔH and SME decreased with increasing ET and SS, RDT was negatively correlated with M_f, M_I, η, G', DSG, and SD, suggesting that rapid and efficient processing promotes greater gelatinization of starch caused microstructural modifications resulting in type V starch diffraction patterns, and an increase in the number of amorphous regions. The highest values of SD (376.26 mg maltose/ g sample), DGS (45.59%), M_f (23.50 N), η (22.76 Pa·s), and RTD (109.46 s), and reduced values of ΔH (0.30 J) and SME (1503.04 kJ·kg^{-1}) were generated at 125 rpm and 129°C. Extruded products under these conditions, and expanded by microwave, showed reductions in SD, DSG, M_f, η, and G', and increases in M_I and G", resulting in snacks with adequate structural characteristics.

Keywords: Extrusion, residence time, microstructural properties, functional properties, third-generation snacks.

Resumen

Este estudio evaluó los efectos de la extrusión y la expansión por microondas sobre las propiedades estructurales de mezclas de arroz, frijoles blancos y pitaya roja en polvo para la producción de botanas de tercera generación. Las mezclas, con un contenido de humedad del 27%, se sometieron a extrusión a diferentes temperaturas (TE; 90, 103, 116 y 129 °C) y velocidades de tornillo (SS; 75, 100 y 125 rpm) y posteriormente a expansión por microondas. Durante la extrusión, se evaluaron el tiempo de residencia (RDT) y la energía mecánica específica, así como el grado de gelatinización del almidón (DSG), la digestibilidad in vitro del almidón (SD), el módulo de almacenamiento (G'), el módulo de pérdida, la viscosidad aparente (η), la relación de expansión (ER), el módulo de flexión (M_f), el momento de inercia (M_I), la entalpía de gelatinización (ΔH) y las propiedades microestructurales de los productos extruidos. ET y SS afectaron significativamente los extruidos y expandidos por microondas. Después de la extrusión, RDT, DSG, SD, η, G', G", M_f, M_I y ER aumentaron, mientras que ΔH y SME disminuyeron con el aumento de ET y SS, RDT se correlacionó negativamente con M_f, M_I, η, G', DSG y SD, lo que sugiere que el procesamiento rápido y eficiente promueve una mayor gelatinización del almidón causando modificaciones microestructurales que resultaron en patrones de difracción de almidón tipo V y un aumento en el número de regiones amorfas. Los valores más altos de SD (376,26 mg de maltosa/g de muestra), DGS (45.59%), M_f (23.50 N), η (22,76 Pa·s) y RTD (109.46 s), y valores reducidos de ΔH (0.30 J) y SME (1503.04 kJ·kg^{-1}) se generaron a 125 rpm y 129 °C. Productos extruidos bajo estas condiciones, y expandidos por microondas, mostraron reducciones en SD, DSG, M_f, η y G', y aumentos en M_I y G", dando como resultado botanas con características estructurales adecuadas.

Palabras clave: Extrusión, tiempo de residencia, propiedades microestructurales, propiedades funcionales, snacks de tercera generación.

*Corresponding author. *E-mail*: aquinter@uach.mx ; https://doi.org/10.24275/rmiq/Alim26706 *ISSN*:1665-2738, *issn-e*: 2395-8472

1 Introduction

Global demand for convenient, shelf-stable, and ready-to-eat food products has increased substantially in recent decades in response to the dynamic pace of modern life and changing dietary preferences (Temgire *et al*., 2021; Tyl *et al*., 2021). Snack foods have emerged as alternatives to satisfy consumer hunger, offering accessible options that are quick to prepare, easy to store, and appealing in flavor and texture (Boukid *et al*., 2022; Serna-Saldivar, 2022). Specifically, third-generation (3G) snacks represent technologically advanced snacks because they combine sensory appeal with innovative processing methods. They can be produced via extrusion cooking, followed by a secondary expansion step involving frying, baking, or microwave heating, to generate a product with an attractive light and crunchy texture. Additionally, diverse flavors can be obtained as they can include a great variety of ingredients and nutritional profiles, including low-fat, gluten-free, or high-protein formulations (Acuario *et al*., 2023; Panak *et al*., 2018; Serna-Saldivar. 2022). The production of 3G snacks is carried out through an extrusion process that operates at high temperatures and short residence times (RDTs). During this process, ingredients such as starches, proteins, and fibers are conveyed through the extrusion barrel via either single- or twin-screw configurations, allowing efficient mixing and cooking (Acuario *et al*., 2023; Panak *et al*., 2018; Serna-Saldivar. 2022). Multiple physicochemical transformations, including starch gelatinization, protein denaturation, water evaporation, Maillard reactions, and amylose-lipid complex formation, occur in the food matrix (Panak *et al*., 2018). These changes during extrusion determine the final texture, functional properties, and retention or degradation of bioactive heat-sensitive components, such as vitamins, antioxidants, and pigments, in the extrudate (Mironeasa *et al*., 2023). Operational parameters, such as temperature, screw configuration and speed, and feed moisture, affect the macromolecules of the food matrix (Alam *et al*., 2016; Castro-Montoya *et al*., 2024; Zambrano *et al*., 2022). These factors are related to RDT and specific mechanical energy (SME), which are critical parameters influencing the efficiency and final quality of extrudates (Kantron *et al*., 2018; Mohamad Mazlan *et al*., 2020; Nwabueze and Iwe, 2010; Wu *et al*., 2023). RDT is defined as the period during which the material is exposed to thermal and mechanical energy inside the extruder; it helps to determine the mechanisms by which energy is transferred to and affects the food matrix throughout the process (Nwabueze and Iwe, 2010; Wu *et al*., 2023). Authors such as Wu *et al*. (2023) and Nwabueze and Iwe (2010) explored the mechanisms by which processing conditions, such as SS, material feeding speed, and material moisture content, affect RDT and reported that shorter processing times generate greater expansion and a lighter texture, whereas longer processing times generate a denser structure and lesser expansion in the textured pea protein and extruded African breadfruit mixtures. Authors such as Ruiz-Gutiérrez *et al*. (2015) reported that short RDTs generated at high temperatures and processing speeds resulted in a high retention of bioactive compounds. On the other hand, Kantron *et al*. (2018) investigated the effects of processing conditions on SME in the production of mushroom-rice extruded products and reported that low feed moisture is the parameter that affects SME the most; low SS increased, whereas high SS reduced SME. Therefore, exploring the RTD of materials within a barrel can provide a better understanding of their mixing and flow status, which is important for controlling the quality of extruded products. The use of proteins in cereal mixtures for the production of extrudates has been previously studied. Authors such as Beltran-Medina *et al*. (2025), García-Cordero *et al*. (2025), Okunola *et al*. (2023) and Pensamiento-Niño *et al*. (2018) studied the changes in the physical and mechanical properties of extruded products using protein-rich snacks based on corn-legumes, rice-cowpea and taro flours and reported that modifications in parameters, such as temperature, SS, and moisture content, significantly affect the final characteristics of the products. However, the combined effects of extrusion temperature and SS on the structural, mechanical, and digestibility properties, RDT, and SME of 3G snacks formulated with rice, white bean, and powdered red pitaya have rarely been investigated to date. Furthermore, the study of these variables and their correlations with changes in macromolecules generated by functional parameters and RDT allow us to understand the ways in which these variables impact the functionality and structure of extruded products. Therefore, this study aimed to evaluate the effects of SS and extrusion temperature on the mechanical, physical, and structural properties and RDT of 3G snacks made with rice, beans, and encapsulated red pitaya.

2 Materials and methods

2.1 Raw materials

Rice and white beans were sourced from a local market in Chihuahua, Mexico. Red pitaya juice (*Stenocereus thurberi*) was obtained from the pitaya fruits collected from Sonora, Mexico and converted to powder via spray drying using a laboratory-scale spray dryer (Yamato ADL311S; Yamato Scientific, Tokyo,

Japan), according to the method of Neder-Suarez *et al*. (2025). The extrusion mixture (rice and white beans) was mixed at a ratio of 90:10 with 10% pitaya powder.

2.2 Flour preparation for extrusion

Rice and white beans were milled in a hammer mill (Pulvex model 200; Mexico) equipped with a 2-mm screen, followed by sieving through the USA standard test sieve (400 μm) to achieve a uniform particle size. The mixture intended for extrusion was adjusted to a moisture content of 27% and stored at 4°C for 12 h prior to processing.

2.3 Extrusion cooking process

The mixture for extrusion was processed using the Shandong Light model LT32L twin-screw extruder at a feed rate of 33.6 g/min. Four extruder barrel temperatures (90, 103, 116, and 129°C) and three SSs (75, 100, and 125 rpm) were used (Table 1). The obtained extrudates were air-dried at 25°C for 24 h. The pellets were expanded via microwave heating with a Hamilton Beach (model HB-P70B20AP-SC) according to the method of Neder-Suarez et al. (2021) to determine the maximum expansion. Times of 17, 20, 23, 26, 29, 32, and 35 s were used. The results indicated that the pellets had the best expansion characteristics at 23 s of treatment time; after 26 s, they showed a brown coloration due to overheating. One portion was stored as a pellet, whereas the other was milled, sieved through the USA standard test sieve (250 μm), and stored at 4°C.

2.4 Residence time distribution (RTD)

The RTD was determined following the method described by Ruiz-Gutiérrez *et al*. (2015), with some modifications. Two grams of the extrusion mixture was mixed with erythrosine (0.1% w/w) and fed into the extruder under process conditions (Table 1). Effluent samples from the extruder were collected every 30 s from time zero until the tracer was no longer detected. The samples were dried at 25 °C for 24 h and then milled and sieved through a USA standard test sieve (400 μm). The a* color parameter was measured to estimate the time distribution. The distribution function E(t) and RTD were calculated via Equations (1) and (2).

$$E(t) = \frac{C(t)}{\int_0^\infty C(t)dt} \tag{1}$$

$$RDT = \int_0^\infty tE(t)dt \tag{2}$$

where C(t) is the tracer concentration (measured as a*) at time (t) and dt is the time interval between successive samplings.

2.5 Specific mechanical energy (SME)

The SME was calculated via the method of Okunola *et al*. (2023). Force measurements taken during the extrusion cooking process of each treatment were used in the calculation, as outlined in Equation (3).

$$SME = \frac{(T * N_s)}{F_t} \tag{3}$$

where T is the torque (Nm), Ns is the SS (1/s), and Ft is the feed flow (kg/h). The SME values are reported in kJ/kg.

2.6 Expansion ratio (ER)

The ER was determined by dividing the diameter of the microwave-expanded product by the diameter of the extruded product (Panak *et al*., 2018). The value was recorded as the average of ten measurements.

2.7 The moment of inertia (M_I) and maximum flexural moment (M_f)

The flexural modulus and moment of inertia of the extruded and microwave-expanded samples were determined following the methods of Aguilar-Palazuelos *et al*. (2007), with some modifications. Tests were conducted via a TA-TX2 texture analyzer (Stable Micro Systems LTD. Surrey, England) with a 25 mm separation in a three-point bending configuration. A compression force was applied at the sample center at a constant speed of 1 mm/min until fracture. The moment of inertia (M_I) and maximum flexural moment (M_f), assuming cylindrical geometry, were calculated via the following equations (4) and (5):

$$M_I = \frac{\pi d^4}{64} \tag{4}$$

$$M_f = \frac{F * L}{4} \tag{5}$$

where F is the maximum force applied at the center of the sample (N), L is the length between the supports of the sample (mm) and d is the diameter of the sample (mm).

2.8 Rheology properties

The rheological behavior of the extrudates was characterized by measuring the G'-storage modulus, G"--loss modulus, and η--apparent viscosity via a rheometer (AR 2000EX, TA Instruments, Crawley, UK) following Neder-Suarez *et al*. (2023). A 25% (w/w, dry basis) suspension was analyzed via a 40 mm stainless-steel parallel plate at 25 °C with a 1500 μm gap. Oscillatory tests were performed from 1–10 Hz at 12% because at this stress a stable viscoelastic response was observed. Flow behavior was assessed

under shear rates of 1–50 1/s, and η at 10 1/s was calculated via the Herschel–Bulkley model. Each treatment was measured four times in accordance with Equation (6).

$$\eta = K\gamma^{n-1} + \frac{\tau}{\gamma} \quad (6)$$

where γ = shear rate (1/s), K = viscosity coefficient (mPa/s), n = fluid behavior index, and τ = yield stress (mPa).

2.9 *Enthalpy of gelatinization*

The enthalpy was determined with a Calorimeter-Q-200 (TA Instruments, Crawley, U.K.). A sample of 10 mg was conditioned with 30 μL distilled water and sealed in hermetically closed aluminum pans. Thermal analysis was performed in the range of 20 °C to 120 °C at a heating rate of 10 °C·min^{-1}. The thermograms obtained were analyzed via Universal Analysis 200 software 4.5 A (TA Instruments, New Castle, DE, USA).

2.10 *Degree of starch gelatinization (DSG)*

The DSG (amylose–iodine complex formation) in extruded and microwave-expanded samples was calculated via the method described by Altan *et al.* (2009), with some modifications. A sample of 1 g was mixed with 50 mL of distilled water and stirred for 10 min in a shaking incubator (Model 1217, Shel Lab, Cornelius, OR, USA) at 25 °C and centrifuged at 3000 × g (Sorvall ST 8R, Thermo Fisher Scientific, Waltham, MA, USA) for 10 min. Subsequently, 1 mL of iodine solution (1%) was added to 1 mL of the resulting supernatant to form a blue amylose-iodine complex. The absorbance (A1) was recorded at 600 nm in a Lambda 25 UV/VIS (PerkinElmer, MA, USA) spectrophotometer. For the raw mixture, 1 g was boiled for 5 min and then diluted to 50 mL. This starch was considered 100% gelatinized, and the absorbance (A2) was recorded. The degree of gelatinization in the extruded samples was calculated as follows the Equation (7).

$$DSG\,(\%) = \frac{A_1}{A_2} \times 100 \quad (7)$$

DGS was reported as the percentage of gelatinized starch. Determinations were performed in triplicate, and the results are expressed as the means ± SDs.

2.11 *In vitro starch digestibility (SD)*

The SD was assessed via the method described by Onyango and Mutungi. (2008),| with some modifications. A portion of 0.4 g of extruded sample was mixed with 25 mL of phosphate buffer at pH 6.9 and 0.5 mL of porcine pancreatic α-amylase solution (40 mg/mL) and then incubated at 37 °C for 2 h in a shaking incubator (Model 1217, Shel Lab, Cornelius, OR, USA). The amount of sugar released was determined with a 540 nm (Lambda 25 UV/VIS; PerkinElmer, MA, USA) spectrophotometer. Starch digestibility was reported as milligrams of maltose per gram of sample. Determinations were performed in triplicate and reported as the mean values ± standard deviation.

2.12 *X-ray analysis*

X-ray diffractograms of mixed, extruded, and microwave-expanded samples were obtained via a Panalytical X'Pert Pro MRD (Malvern, U.K.) according to Neder-Suarez *et al.* (2021). The data were collected from 5° to 30° (2θ) at a step size of 0.5°·s^{-1} and analyzed with OriginPro 9.0 software.

2.13 *FT-IR analysis*

FT-IR spectra of the mixture, extrudate, and microwave-expanded samples were recorded via an ATR-FTIR spectrometer (PerkinElmer, Norwalk, USA) over the 4000–650 cm^{-1} range, with a resolution of 4 cm^{-1} and ten scans per sample.

2.14 *Scanning electron microscopy*

The raw material, mixture, extrudate, and microwave-expanded samples (<74 μm) were analyzed via SEM (JSM-5800LV, JEOL, Japan) at 10 kV via a secondary electron detector. The samples were gold-coated under high vacuum (Desk II, Denton) and magnified to 800x. The particle size was measured with ImageJ v1.50i (NIH, USA).

2.15 *Experimental Design and Statistical Analysis*

A duplicate factorial design was used. Four levels of temperature and three screw speeds were varied, resulting in 12 treatments. The data were analyzed via ANOVA and Pearson's correlation ($p < 0.05$) via Minitab® 17.1.0 (Minitab Inc., State College, PA, USA). Differences were considered statistically significant at $p < 0.05$ according to Tukey's test.

3 Results and discussion

3.1 *Residence time (RTD)*

RTD values of the extruded products were significantly affected by both SS and ET. This parameter is critical because it affects the duration of exposure to heat, pressure, and mechanical shear,

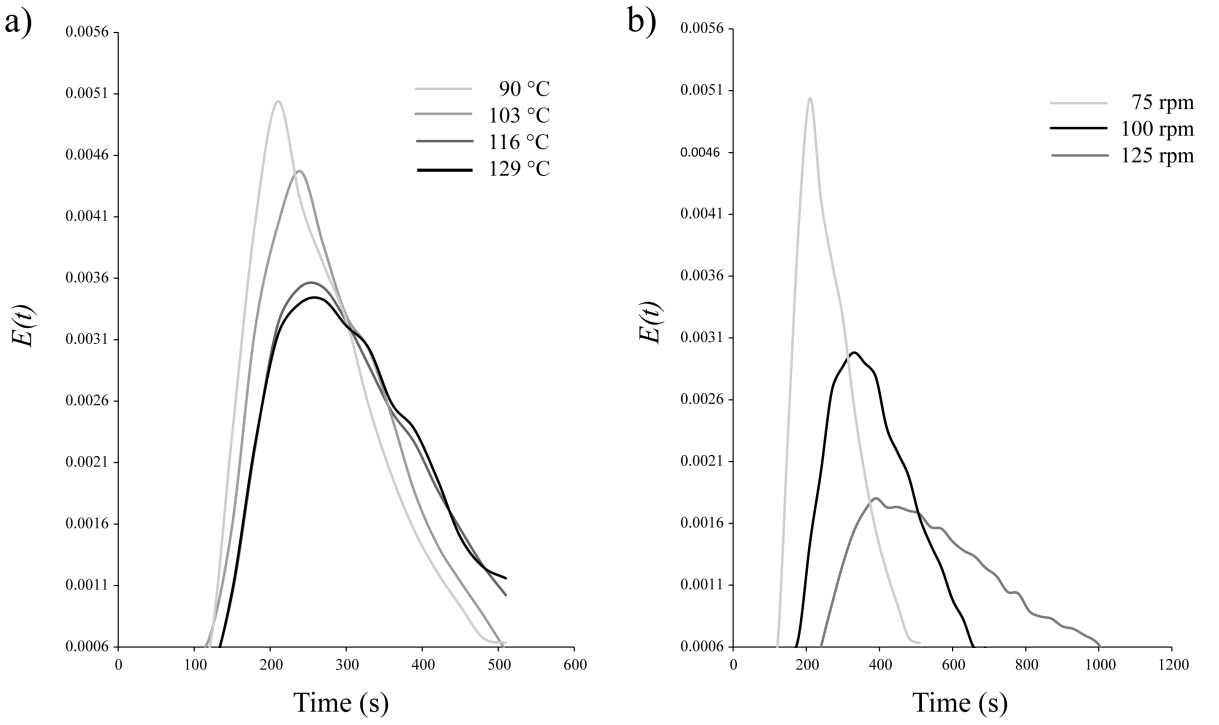

Figure 1. Residence time distribution (RTD) under different processing conditions: (a) screw speed effect and (b) barrel temperature effect.

which affects the cooking time, texture, and nutritional properties of the extruded product (Nwabueze & Iwe, 2010; Wu *et al*., 2023). Our results indicate that a reduction in RDT causes noticeable changes in starch by increasing the degree of starch gelatinization (DSG), SD, and rheological properties, in addition to improving the mechanical strength of the products and reducing SME during processing. An increase in SS reduced the RDT values at all temperatures (Table 1), indicating major transit of the material through the extruder due to the increased mechanical force. At a constant processing speed, an increase in temperature increases the RTD (Figure 1a), possibly due to a decrease in the viscosity of the material, which can decrease the efficiency of transport by the screw, favoring partial retreat or formation of dead zones where the material accumulates (Chuang & Yeh, 2004), as the screws used did not have backflow restrictors (Figure S1). The highest RTD was observed at 129°C and 75 rpm (Table 1), suggesting prolonged exposure to thermal and mechanical inputs, which was significantly different from those in the other treatments. In contrast, the lowest RTD was noted at 90°C and 125 rpm, which resulted in minimal residence time and reduced processing intensity. An increase in SS at any temperature decreased the RTD (Figure 1b) due to the increased shear and conveying efficiency rates, which reduce material retention within the barrel (Nwabueze & Iwe, 2010; Ruiz-Gutierrez *et al*., 2015; Wu *et al*., 2023). Additionally, according to the configuration of the screws (Figure S1), which do not restrict flow, the blades were single-pass and contained spaces to favor the displacement of the material. The flow of the solid was limited only by the corrosive effect of the screws; therefore, RTD was affected only by SS, which is the dominant factor impacting RDT and directly impacting physicochemical transformations during extrusion. The barrel temperature had a less pronounced effect (Figure 1b); at high ETs, this effect can be related to changes in material plasticization and increase in melt viscosity and pressure, which influence the flow behavior and residence time (Alam *et al*., 2016; Kantrong *et al*., 2018; Wang *et al*., 2022). These effects can be observed in the changes in the degree of gelatinization and viscosity of the products, with a decrease in RDT increasing the degree of gelatinization and viscosity of the products and decreasing the enthalpy.

3.2 SME

SME represents the energy supplied to the material by the mechanical action of the extruder screws, which affects the efficiency of the process during extrusion (Mohamad *et al*., 2020; Pensamiento-Niño *et al*., 2018). SME was significantly affected by both SS and ET. At 90°C and 75 rpm (Table 1), SME was the highest during the process, as a lower SS increases the shear pressure inside the barrel, which increases the torque requirements, generating a positive correlation with RDT ($r = 0.69$; $p < 0.01$). The increased

residence time results from a lower SS, which also causes greater resistance to material flow and higher torque, thereby increasing the energy consumption. Additionally, a lower ET generated higher SME values at the same SS, suggesting greater mechanical work, which increases the resistance to flow and material viscosity (Aguilar-Palazuelos *et al*., 2011; Singha *et al*., 2018). Authors such as Mohamad Mazlan *et al*. (2021) and Kantron *et al*. (2018) reported that an increase in barrel temperature decreases SME in the production of corn–mango peel and mushroom–rice snacks. SME decreased as SS increased, and the lowest SME was observed at 129°C and 125 rpm (T3). A higher SS reduces the energy transfer per unit mass and decreases the residence time and shear intensity (Alam *et al*., 2016; Nwabueze & Iwe, 2010; Wu *et al*., 2023). The increase in ET from 90°C to 129°C at a constant SS resulted in a reduction in SME; this is likely due to the decrease in melt viscosity at higher temperatures, which results in a lower resistance to flow and reduces the mechanical energy required during extrusion (Mohamad *et al*., 2020; Okunola *et al*., 2023; Pensamiento-Niño *et al*., 2018; Singha *et al*., 2018). Similar results have been reported by Altan *et al*. (2008) for barley flour-based extruded products and Neder-Suarez *et al*. (2022) for 3G snacks made from blue corn, black bean, and chare.

3.3 Expansion ratio (ER)

The quality of expanded products made from 3G snacks is a quality parameter for consumer acceptance (Alam *et al*., 2016). ER was significantly affected by ET and SS. The highest ER was observed for the products extruded at high ETs and SSs (Figure S2), reaching a maximum value of 2.02 (T3; $p < 0.05$). This is attributed to the greater starch modification during extrusion, resulting in a flexible and porous matrix with higher bound water content, which promotes efficient expansion during microwave heating and enhances the mechanical strength of the final product (Van der Sman & Bows, 2017; Zambrano *et al*., 2022). This is consistent with the results of Pearson analysis, which revealed that ER was positively correlated with DSG ($r = 0.88$; $p < 0.01$) and flexural modulus (M_f; $r = 0.83$; $p < 0.01$), suggesting that greater starch gelatinization enhances expansion and mechanical strength. Conversely, the negative correlation with enthalpy ($r = –0.80$; $p < 0.01$) suggested that lower gelatinization promotes the expansion efficiency and structural stability of the extruded products. Authors such as Gümüşaya and şeker (2021) indicated that an adequate degree of gelatinization to generate good expansion is above 50%. On the other hand, products extruded at low ETs exhibit low ERs (Table 2) because of incomplete gelatinization and more compact matrices (Zhang *et al*., 2021).

3.4 Moment of inertia (M_I) and flexural modulus (M_f)

M_f and M_I values of the extruded and microwave-expanded samples are shown in Table 1. These parameters are indicators of mechanical integrity and internal structure, providing information on the texture and crispness of the extruded and expanded products (Delgado-Nieblas *et al*., 2021). M_f and M_I values were significantly affected ($p < 0.05$) by ET and SS after extrusion and microwave expansion. After the extrusion process, the highest values of M_f and M_I were noted at 129°C and 125 rpm (T3), which were significantly higher than those in the other treatments; this increase was due to high temperatures and SSs increasing starch gelatinization and protein denaturation, which promoted the major expansion of the extrudates (Qui *et al*., 2024). This expansion caused the material to acquire a more resistant and uniform structure as SS increased, thereby increasing the M_I and mechanical resistance. M_f was positively correlated with DSG ($r = 0.97$; $p < 0.01$) and M_I ($r = 0.98$; $p < 0.01$), suggesting that greater gelatinization generates more cohesive and resistant structures, improving the ability of the material to resist stress and distribute internal stress more effectively. Additionally, RTD was negatively correlated with M_I ($r = –0.76$; $p < 0.01$) and M_f ($r = –0.88$; $p < 0.01$), suggesting that low RTD favors more expanded products. Moreover, the lowest values of M_f and M_I were observed at 90°C and 75 rpm, indicating the insufficient gelatinization of starch, which reduced the formation of a cohesive structural matrix and negatively affected the mechanical integrity of the extrudate, generating a weak and poorly developed internal network (Zhang *et al*., 2021). After the microwave expansion process, the M_I values increased and M_f values decreased, with the highest M_I value observed for T3 (Table 1), which was significantly different from those in the other treatments. An increase in ET at the highest SS increased M_I, thereby improving starch gelatinization, which enabled the extruded material to acquire a more resistant structure with greater expansion. The increase in M_I after the microwave expansion process was due to the increase in the volume of the snack, which generated a more open but solid structure. As a result, the mass was distributed further from the axis, resulting in a greater M_I. However, M_f decreased in the extruded products (Table 1) because the inflated snack became more porous, exhibited a lower density, and was fragile, showing decreased resistance to bending despite the greater volume obtained due to the loss of structural rigidity (Lisiecka *et al*., 2021; Van der Sman & Bows, 2017; Zambrano *et al*., 2022). Similar results have been reported by Tyl *et al*. (2023) and Lisiecka *et al*. (2021) for branch-enriched extruded and potato-based snacks, suggesting that expansion reduces the

mechanical strength of products.

3.5 Rheology properties

The rheological behavior of the extruded samples was significantly affected ($p < 0.05$) by ET and SS. The apparent viscosity (η), storage modulus (G'), and loss modulus (G") increased with increasing SS and ET after extrusion. At high temperatures and SSs, the highest η values were obtained (Table 1). The highest viscosity was noted at 129°C and 125 rpm (T3), which was significantly different ($p < 0.05$) from those recorded in other treatments. Viscosity increased with increasing temperature at constant SS (Table 1), which is attributed to the greater gelatinization and melting of starch components and partial denaturation of proteins (Alam *et al*., 2018; Onyango *et al*., 2022; Zambrano *et al*., 2022). η was negatively correlated with the enthalpy of gelatinization (ΔH; $r = –0.91$; $p < 0.01$), suggesting that materials with lower enthalpy exhibit higher viscosity. On the other hand, the lowest viscosity was observed at a low temperature and SS (T10), generating the highest enthalpy and lowest DSG, and viscosity reduction increased SME and reduced RDT (Kantrong *et al*., 2018). A similar trend was observed for the storage modulus, which increased at higher SSs and different ETs. The highest G' value was recorded at 90°C and 125 rpm, and the values were significantly different ($p < 0.05$). This behavior may be due to starch-protein interactions and amylose-lipid complex formation under intense mechanical shear or starch retrogradation, resulting in elastic gel behavior in the extrudates (Alam *et al*., 2016; Wang *et al*., 2022). RTD was negatively correlated with η ($r = –0.80$; $p < 0.01$) and G' ($r = –0.72$; $p < 0.01$), suggesting that lower RTD generates products with greater molecular integrity. Additionally, lower ETs and SSs reduced the η and G' values, possibly due to partial gelatinization or insufficient protein denaturation, limiting the formation of a solid structural network (Singh *et al*., 2019). G" values of the samples subjected to 100 rpm treatment were the highest, followed by a decrease at 125 rpm, which indicates that the material is more viscous in an elastic-dominated system as SS increases the degree of formation and structural rigidity of the extrudates (Wang *et al*., 2023). After expansion of the extruded products via microwave heating, their rheological parameters were significantly affected ($p < 0.05$) by ET and SS. η values of the expanded products were lower than those of the extruded products (Table 2); this reduction occurs because, during heating, water in the system heats, causing starch gelatinization, thermal hydrolysis, and breaking of hydrogen bonds in the starch structure during processing, resulting in a lower viscosity (Onyango *et al*., 2022; Oyeyinka *et al*. 2021; Wang *et al*., 2023; Zambrano *et al*., 2022). η was positively correlated with G' ($r = 0.97$; $p < 0.01$), suggesting that greater flow resistance leads to higher elastic energy storage. The highest η and G' values were observed at high ETs and SSs, and a reduction in ET and SS resulted in lower values.

3.6 ΔH

ΔH reflects the degree of crystalline order in starch, indicating the energy required to disrupt this structure; higher values of ΔH correspond to a greater proportion of ordered crystalline structures (Cooke & Gidley, 1992). ΔH was significantly affected by ET and SS during the extrusion process. ΔH decreased with increasing SS at all temperatures (Table 1), indicating greater starch gelatinization and molecular disruption due to the increased mechanical shear and pressure generated during the process (Jia *et al*., 2023; Qiu *et al*., 2024). The highest ΔH value was noted at low temperatures, and, at a lower SS (T10), it was significantly different ($p < 0.05$) from those in the other treatments. ΔH was positively correlated with RDT ($r = 0.56$; $p < 0.01$), and RDT reduction generated a decrease in ΔH with major gelatinization and rupture of the crystalline structure of starch due to exposure time to heat and pressure conditions in the extruder (Nwabueze & Iwe, 2010; Wu *et al*., 2023). The ΔH value was negatively correlated with SD ($r = –0.79$; $p < 0.01$), suggesting that a relatively high value of ΔH makes the starch more accessible for enzymatic hydrolysis, generating relatively high values of SD (Qiu *et al*., 2024). These results are similar to those reported by Jia *et al*. (2023) for extruded products based on wheat semolina, where an increase in SS results in a reduction in ΔH. On the other hand, ΔH was positively correlated with SME ($r = 0.91$; $p < 0.01$), as the major mechanical energy generated by a higher SS result in modifications in starch structures, such as gelatinization or dextrinization, which reduces the enthalpy.

3.7 DSG

DSG is a critical parameter of extruded products that influences their functional, nutritional, and textural properties. DSG was used to evaluate the mechanism by which the native crystalline material transforms into an amorphous state due to the processing conditions (Huang *et al*., 2022; Jia *et al*., 2014). DSG values of the extruded and microwave-expanded products were significantly affected by ET and SS. DSG values ranged from 15.01% to 44.99%. The highest value of DSG was observed at 129°C and 125 rpm (Table 1) due to the combination of thermal energy and shear stress generated by higher SSs, resulting in granule swelling, rupture of the granular structure of starch, and gelatinization (Alam *et al*., 2016; Altan *et al*., 2008). DSG

was positively correlated with η (r = 0.95; p < 0.01), indicating greater transformation of starch granules into an amorphous state, which results in greater water absorption and paste properties of gelatinized starch (Altan *et al*., 2008; Okanola *et al*., 2023; Zambrano *et al*., 2024). On the other hand, lower values of DSG were observed at lower TEs and SSs (Table 1). The lowest DSG value was noted at 90°C and 75 rpm (T10), which was significantly different (p < 0.05) from those recorded in the high-SS and high-ET treatments, suggesting that insufficient thermal and mechanical energy was applied for the gelatinization of starch granules (Alam *et al*., 2016; Qiu *et al*., 2024). RTD was negatively correlated with DSG (r = –0.78; p < 0.01), indicating lower thermal and mechanical efficiencies. However, an increase in SS increases DSG, which further increases mechanical shear, resulting in molecular mobility and greater gelatinization of starch (Ali *et al*., 2008; Huang *et al*., 2022). After the microwave expansion process, DSG was significantly affected by ET and SS, showing a decrease in value (Table 1). This decrease may be due to microwave energy causing internal water evaporation, inducing the expansion of products with partially gelatinized degraded amorphous starch, promoting retrogradation, and inducing recrystallization with more ordered structures, thereby lowering the DSG values (González-Soto *et al*., 2021; Zuo *et al*., 2022). A similar DSG trend was observed after extrusion, with the highest TEs and SSs resulting in maximum DSG values after the microwave expansion of products. In contrast, lower ETs combined with low SSs resulted in minimal DSG values (Table 1) due to the incomplete gelatinization of starch granules during extrusion (Chuang & Yeh, 2004; Jia *et al*., 2021).

3.8 In vitro starch digestibility (SD)

SD measures the enzymatic conversion of starch to glucose under simulated digestive conditions, indicating its nutritional and glycemic effects (Ali *et al*., 2019; Huang *et al*., 2022). The unprocessed mixture exhibited an SD value of 70.40 ± 2.78 mg maltose/g sample d.b. SD values of the extruded and microwave-expanded products were significantly affected by ET and SS. After the extrusion process, SD values of all the samples increased from 300 to 376 mg maltose/g sample d.b. (Table 1). SD values significantly increased with increasing TEs and SSs, reaching maximum values at 125 rpm and 129°C (T3). These high values were due to the major gelatinization and reduction in starch crystalline regions during processing. This phenomenon, due to high temperatures, pressures, and shear stress, increases the amylolytic enzymatic attack on the amorphous starch matrix, resulting in higher levels of digestible starch (Huang *et al*., 2022; Wang *et al*., 2023). Wang *et al*. (2023) and Jan *et al*. (2025) reported similar values for extruded products made from corn and rice starch. RTD was negatively correlated with SD (r = –0.76; p < 0.01), suggesting greater digestibility at a lower RTD because the thermal conditions and shear forces are adequate for gelatinization and dextrinization, which increase digestibility. In contrast, lower ETs and SSs during extrusion yielded lower SD values (Table 1), indicating a lower DSG, which preserved the granular integrity, thereby limiting starch hydrolysis during digestion. SD was positively correlated with DSG (r = 0.96; p < 0.01), suggesting that highly gelatinized starch is more accessible for enzymatic hydrolysis, thereby improving digestibility (Ali *et al*., 2008). After the microwave expansion process, starch digestibility decreased. The highest SD value was observed at 129°C and 125 rpm, which was significantly different (p < 0.05) from those in the other treatments, whereas the lowest values were observed at low SSs (Table 1). SD was positively correlated with DSG (r = 0.95; p < 0.01) after the microwave expansion process, indicating that it promoted retrogradation, resulting in more ordered crystalline structures that were less accessible to digestive enzymes, thereby reducing the SD value.

3.9 X-ray analysis

X-ray diffraction analysis revealed the structural modifications in a rice-bean mixture subjected to extrusion processing, as influenced by ET and SS. The unprocessed mixture exhibited an A-type crystalline pattern, characterized by peaks at 2θ angles of 15.1°, 17.2°, 18.1°, and 22.8° (Figure 2a). This pattern is common in starches sourced from cereals, such as corn, wheat, and rice, and associated with their crystalline structure (Liu *et al*., 2024; Wang *et al*., 2023; Wu *et al*., 2020). The presence of these peaks indicates high crystallinity, primarily characterized by a high-intensity peak at 22.8° (46.03%), which is related to thermal stability (Liu *et al*., 2024). After the extrusion process, the samples showed a reduction in crystallinity at 15.1° and 17.2°, indicating partial disruption of the native starch crystallites and partial gelatinization due to the combined effects of high thermal and mechanical shear. New diffraction peaks were observed at 2θ values of 12.8° and 19.8° (Figure 2b), indicating the presence of a V-type crystalline pattern with the formation of amylose–lipid complexes and partial retrogradation and molecular reorganization during processing due to high shear and thermal conditions (Liu *et al*., 2024; Wang *et al*., 2023). This indicates the destruction of original crystal structures and promotion of new crystalline arrangements. In general, the increase in SS at high ET resulted in a decrease in the 15.1° and 22.8° angles (Table 3), with the most significant decrease

observed in T3, suggesting that starch undergoes greater gelatinization and molecular disorganization under more intense conditions. Similarly, the new diffraction peaks at 12.8° and 22.8° were larger at high SS values (Figure 2), indicating recrystallization after processing.

Table 1. Mechanical, physical and rheological properties of extruded products.

T	ET	SS	RTD	SME	DGS	SD	M_f	M_I	ΔH	η	G'	G"
1	129	75	259.39 ± 6.99^{a}	1889.10 ± 55.60^{d}	15.01 ± 0.21^{e}	335.62 ± 3.43^{b}	1.62 ± 0.31^{f}	9.44 ± 1.02^{f}	0.810 ± 0.056^{c}	7.26 ± 0.41^{ef}	181.82 ± 2.93^{d}	145.25 ± 3.47^{c}
2	129	100	146.64 ± 5.95^{c}	1589.30 ± 24.60^{fg}	19.47 ± 1.15^{cd}	342.31 ± 3.42^{b}	3.20 ± 0.10^{cd}	14.18 ± 0.74^{de}	0.346 ± 0.020^{e}	12.27 ± 0.62^{d}	264.82 ± 10.02^{b}	189.68 ± 14.13^{a}
3	129	125	109.46 ± 6.49^{de}	1503.04 ± 12.32^{g}	45.59 ± 0.55^{a}	376.26 ± 7.20^{a}	5.69 ± 0.36^{a}	23.50 ± 1.17^{a}	0.300 ± 0.015^{e}	22.76 ± 1.86^{a}	307.30 ± 30.60^{a}	110.46 ± 10.40^{de}
4	116	75	235.80 ± 6.84^{b}	2086.20 ± 18.80^{c}	12.91 ± 1.54^{ef}	326.42 ± 3.48	1.61 ± 0.31^{f}	9.29 ± 0.46^{fg}	0.835 ± 0.085^{c}	6.13 ± 0.57^{fg}	150.16 ± 2.71^{e}	140.37 ± 6.02^{c}
5	116	100	140.19 ± 4.61^{c}	1782.30 ± 20.35^{e}	21.25 ± 0.35^{c}	343.79 ± 3.59^{b}	2.79 ± 0.24^{e}	13.33 ± 1.26^{e}	0.507 ± 0.030^{d}	12.25 ± 0.37^{d}	253.23 ± 8.20^{bc}	177.61 ± 2.03^{ab}
6	116	125	114.69 ± 6.62^{d}	1507.15 ± 14.23^{fg}	43.86 ± 0.39^{a}	373.02 ± 7.34^{a}	4.48 ± 0.52^{b}	22.26 ± 1.99^{ab}	0.580 ± 0.063^{d}	19.34 ± 1.39^{b}	272.45 ± 7.67^{b}	120.20 ± 7.35^{de}
7	103	75	227.70 ± 1.55^{b}	2217.60 ± 53.70^{b}	11.82 ± 0.62^{f}	328.44 ± 2.63^{b}	1.76 ± 0.35^{f}	9.92 ± 0.82^{f}	1.247 ± 0.042^{b}	3.74 ± 0.20^{gh}	34.35 ± 8.87^{f}	46.47 ± 1.85^{f}
8	103	100	143.18 ± 5.10^{c}	1790.50 ± 43.30^{de}	19.72 ± 0.49^{cd}	342.42 ± 4.12^{b}	3.41 ± 0.13^{c}	15.56 ± 1.28^{d}	0.931 ± 0.015^{c}	11.83 ± 0.76^{d}	245.91 ± 11.56^{bc}	167.20 ± 6.39^{b}
9	103	125	98.66 ± 3.08^{de}	1609.80± 18.80^{f}	39.57 ± 0.14^{b}	367.04 ± 6.40^{a}	4.55 ± 0.39^{b}	20.21 ± 1.10^{c}	0.638 ± 0.033^{d}	16.02 ± 0.87^{c}	266.95 ± 5.42^{b}	120.17 ± 4.54^{de}
10	90	75	215.73 ± 4.10^{b}	2340.80 ± 32.60^{a}	7.24 ± 0.28^{g}	300.73 ± 2.69^{c}	1.43 ± 0.07^{f}	7.94 ± 0.92^{g}	1.623 ± 0.129^{a}	2.87 ± 0.29^{h}	35.78 ± 4.54^{f}	49.70 ± 4.95^{f}
11	90	100	115.51 ± 6.84^{de}	2045.10 ± 56.50^{c}	17.69 ± 1.70^{d}	333.84 ± 9.38^{b}	2.93 ± 0.16^{de}	13.61 ± 0.83^{e}	1.217 ± 0.085^{b}	9.12 ± 0.43^{e}	189.43 ± 4.85^{d}	132.39 ± 4.50^{cd}
12	90	125	89.75 ± 7.98^{e}	1720.70 ± 25.60^{e}	38.88 ± 0.32^{b}	373.27 ± 2.13^{a}	4.57 ± 0.30^{b}	21.19 ± 2.53^{bc}	0.578 ± 0.034^{d}	15.63 ± 0.81^{c}	226.19 ± 7.71^{c}	103.19 ± 3.70^{e}

Average values in each column with different letters represent a significant difference according to the Tukey test (α = 0.05). T= treatments, ET = extrusion temperature (°C), SS = screw speed (rpm), RT = residence time (s), SME = specific mechanical energy (kJ·kg^{-1}), DGS = degree of starch gelatinization (%), SD = *In vitro* starch digestibility (mg maltose/ g sample), M_f = maximum flexural moment (N), M_I = moment of inertia (mm^4), ΔH = enthalpy (J), η = apparent viscosity (Pa·s), G' = storage module (Pa) and G" = loss modulus (Pa)

Table 2. Mechanical, physical and rheological properties of microwave-expanded products.

T	ET	SS	DGS	SD	M_f	M_I	ΔE	ER	η	G'	G"
1	129	75	13.19 ± 0.35^{f}	321.91 ± 6.74^{ef}	5.03 ± 0.62^{ef}	9.89 ± 0.98^{ef}	40.70 ± 0.36^{cd}	1.58 ± 0.05^{def}	4.11 ± 0.26^{g}	110.25 ± 11.63^{f}	110.35 ± 10.24^{e}
2	129	100	18.16 ± 0.90^{d}	338.33 ± 5.14^{cd}	6.32 ± 1.18^{cd}	18.08 ± 4.24^{d}	39.79 ± 0.31^{e}	1.63 ± 0.05^{de}	7.49 ± 0.22^{e}	317.02 ± 4.23^{d}	283.57 ± 8.18^{a}
3	129	125	40.74 ± 1.65^{a}	354.62 ± 7.12^{ab}	10.24 ± 1.37^{a}	77.13 ± 6.36^{a}	41.40 ± 0.55^{bc}	2.02 ± 0.06^{a}	19.58 ± 0.61^{a}	551.45 ± 9.67^{a}	226.65 ± 2.96^{c}
4	116	75	8.84 ± 0.28^{g}	314.17 ± 1.07^{f}	5.14 ± 0.81^{def}	8.526 ± 1.61^{f}	40.68 ± 0.35^{cd}	1.55 ± 0.09^{ef}	1.97 ± 0.05^{h}	55.23 ± 1.37^{g}	54.64 ± 2.29^{f}
5	116	100	16.07 ± 0.42^{de}	325.45 ± 2.70^{def}	5.94 ± 0.48^{cde}	18.65 ± 4.16^{d}	39.78 ± 0.34^{e}	1.54 ± 0.07^{ef}	3.92 ± 0.26^{g}	117.70 ± 8.32^{f}	117.5 ± 6.93^{e}
6	116	125	41.97 ± 0.98^{a}	362.55 ± 4.43^{a}	9.19 ± 1.53^{a}	58.89 ± 9.36^{b}	42.11 ± 0.33^{a}	1.81 ± 0.05^{b}	16.6 ± 0.69^{b}	457.60 ± 22.4^{b}	191.95 ± 5.94^{d}
7	103	75	8.66 ± 0.36^{g}	319.32 ± 2.29^{ef}	5.22 ± 0.55^{de}	5.628 ± 0.47^{f}	39.73 ± 0.29^{e}	1.34 ± 0.05^{h}	1.24 ± 0.07^{h}	13.12 ± 1.08^{h}	13.04 ± 1.81^{g}
8	103	100	14.87 ± 0.61^{ef}	341.20 ± 1.56^{bcd}	7.01 ± 0.48^{bc}	14.98 ± 1.89^{de}	40.01 ± 0.10^{d}	1.45 ± 0.03^{g}	9.54 ± 0.61^{d}	301.02 ± 5.54^{d}	256.72 ± 8.68^{b}
9	103	125	38.26 ± 0.43^{b}	350.90 ± 5.59^{abc}	7.94 ± 0.96^{b}	35.77 ± 7.42^{c}	41.35 ± 0.40^{b}	1.67 ± 0.07^{cd}	13.59 ± 0.48^{c}	400.42 ± 9.13^{c}	218.53 ± 4.49^{c}
10	90	75	5.97 ± 0.98^{h}	318.52 ± 5.23	4.06 ± 0.58^{f}	4.70 ± 0.81^{f}	39.82 ± 0.36^{e}	1.34 ± 0.05^{h}	1.59 ± 0.14^{h}	22.69 ± 1.79^{h}	24.463 ± 1.76^{g}
11	90	100	14.63 ± 0.20^{ef}	332.12 ± 9.13^{de}	5.23 ± 0.76^{de}	15.27 ± 2.40^{de}	40.71 ± 0.34^{d}	1.51 ± 0.05^{fg}	5.64 ± 0.26^{f}	206.63 ± 6.37^{e}	190.82 ± 6.64^{d}
12	90	125	34.96 ± 1.28^{c}	352.04 ± 5.63^{abc}	7.88 ± 1.11^{b}	38.58 ± 5.26^{c}	40.67 ± 0.24^{cd}	1.72 ± 0.08^{bc}	12.55 ± 0.41^{c}	420.32 ± 12.09^{c}	191.55 ± 3.56^{d}

Average values in each column with different letters represent a significant difference according to the Tukey test (α = 0.05). T= treatments, ET = extrusion temperature (°C), SS = screw speed (rpm), DG = degree of starch gelatinization (%), SD = *In vitro* starch digestibility (mg maltose/ g sample), M_f = maximum flexural moment (N), M_I = moment of inertia (mm^4), ΔE = color change, ER = expansion radius, η = apparent viscosity (Pa·s), G' = storage module (Pa) and G" = loss modulus (Pa)

Table 3. FTIR absorbance values and the percentage of relative of product extrudates.

			IR ratios		Percentage of relative crystallinity at 2θ					
Treatment	ET	SS	1047/1022	1022/995	12.8°	15.1°	17.2°	18.1°	19.8°	22.8°
1	129	75	2.90	1.54	7.68	19.84	10.20	12.54	22.17	27.55
2	129	100	2.78	1.48	12.80	13.69	9.38	12.19	25.49	26.42
3	129	125	2.58	1.36	18.53	9.29	7.02	11.84	32.86	17.73
4	116	75	2.80	1.55	9.74	14.21	7.39	10.93	23.22	34.48
5	116	100	2.61	1.49	12.64	16.18	8.95	11.56	26.32	24.33
6	116	125	2.56	1.51	15.45	13.53	7.15	11.26	29.31	23.98
7	103	75	2.59	1.58	14.09	24.00	6.57	11.83	14.76	28.73
8	103	100	2.35	1.45	19.08	18.58	9.77	9.35	21.04	22.15
9	103	125	2.40	1.49	20.31	17.14	13.78	5.81	27.45	18.48
10	90	75	2.44	1.61	4.50	18.10	9.77	13.28	21.52	36.92
11	90	100	2.36	1.47	12.56	15.76	11.64	12.38	23.29	24.50
12	90	125	2.57	1.49	16.30	14.97	10.48	11.73	26.23	21.16
Mixture			2.12	1.75	N/D	31.56	14.64	7.75	N/D	46.03

ET = extrusion temperature (°C), SS = screw speed (rpm), Mixture = 90:10 rice and white beans, N/D = not detected

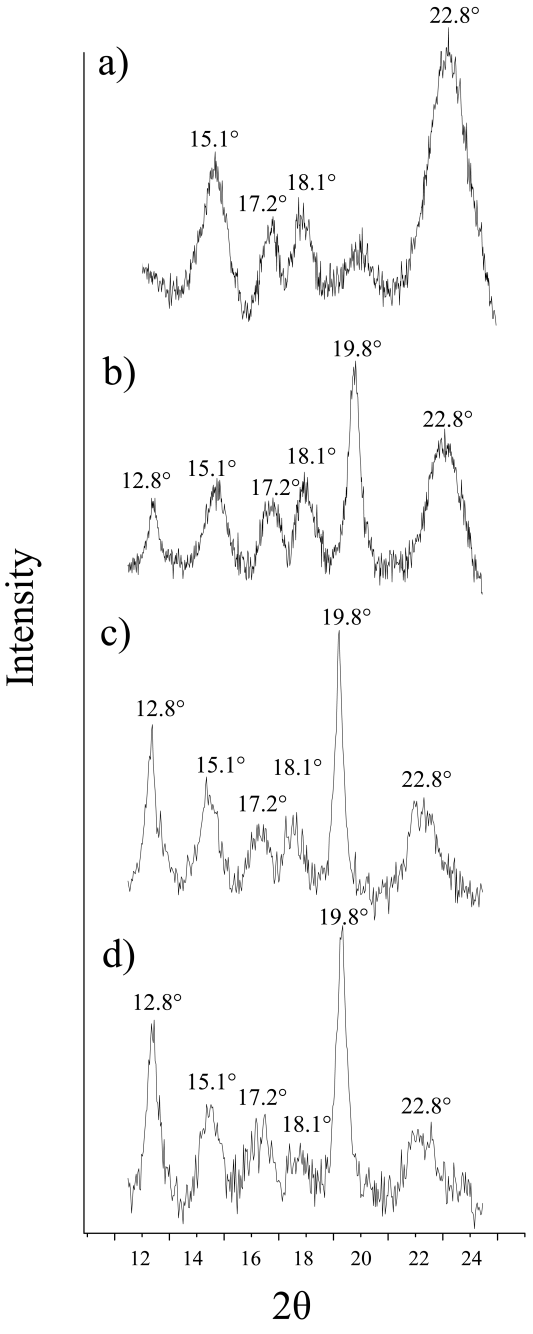

Figure 2. X-ray spectra: a) raw material, b) sample extruded at low screw speed (75 rpm), B) sample extruded at intermediate screw speed (100 rpm) and c) sample extruded at high screw speed (125 rpm).

3.10 Fourier-transform (FT)-infrared (IR) analysis

FT-IR spectroscopy was used to evaluate the changes in the molecular organization of macromolecules, such as starch, after thermal processing. Specific wavelengths, such as 1047 cm^{-1}, are associated with vibrations of C–O bonds in ordered or crystalline structures, and 1022 cm^{-1} is associated with the less organized or amorphous regions of starch (Liu *et al*., 2024; Wu *et al*., 2020). A ratio of 1047/1022 or short crystallinity index reflects the degree of crystallinity, with high values indicating increased crystallinity (Jia *et al*., 2023; Liu *et al*., 2024; Lu *et al*., 2021). Conversely, a ratio of 1022/995 or structural disorders and high values are associated with increased amorphous content (Huang *et al*., 2023; Wu *et al*., 2020). The values for the raw mixtures are shown in Table 3. During extrusion, thermal and mechanical conditions led to starch gelatinization and disruption of its native crystalline structure. However, in extruded products with complex mixtures of starch and proteins, an increase in FT-IR absorbance at a ratio of 1047/1022 and decrease in the ratio of 1022/995 were observed compared to those in unprocessed materials (Liu *et al*., 2024; Wu *et al*., 2020; Zhang *et al*., 2023). The IR ratio (1047/1022) decreased with increasing ET and SS, indicating the loss of crystalline order. This behavior was attributed to the formation of new semi-ordered structures (Table 3), particularly V-type amylose–lipid or amylose–protein complexes, promoted by the interaction between high-amylose rice starch and lipids or proteins naturally present in beans. These V-type structures, although distinct from native A-type crystalline structures, contribute to a relative increase in the 1047 cm^{-1} band and reduction in the 1022 cm^{-1} band, reflecting the amorphous starch regions, and a relative increase in the 995 cm^{-1} band, indicating more hydrogen-bonded C–OH groups, resulting in a low ratio of 1022/995 (Liu *et al*., 2024; Wang *et al*., 2020; Wu *et al*., 2020). The ratio of 1022/995 decreased with increasing SS (Table 3), disrupting the molecular order due to starch gelatinization and partial depolymerization by high temperature, breaking hydrogen bonds, and destabilizing the double helix structure, thereby increasing the amorphous state. These changes in the food matrix composition determine the final structure of extruded products.

3.11 Scanning electron microscopy

Micrographs revealed clear distinctions in the surface morphology and structural characteristics of the raw ingredients, extruded products, and microwave-expanded samples. Figure 3a shows the unprocessed white rice with a semispherical shape and amorphous granules with a coarse surface and an average size of 25 μm, similar to the values reported by Govindaraju *et al*. (2019) and Zhang *et al*. (2023). This type of morphology is typical of unprocessed cereal starches, which are known for their compound granules with irregular shapes and relatively low crystallinity and molecular order. In contrast, Figure 3b shows that the bean starch granules of raw bean products, which are spherical or ellipsoid, exhibit a more defined shape with larger and elongated dimensions

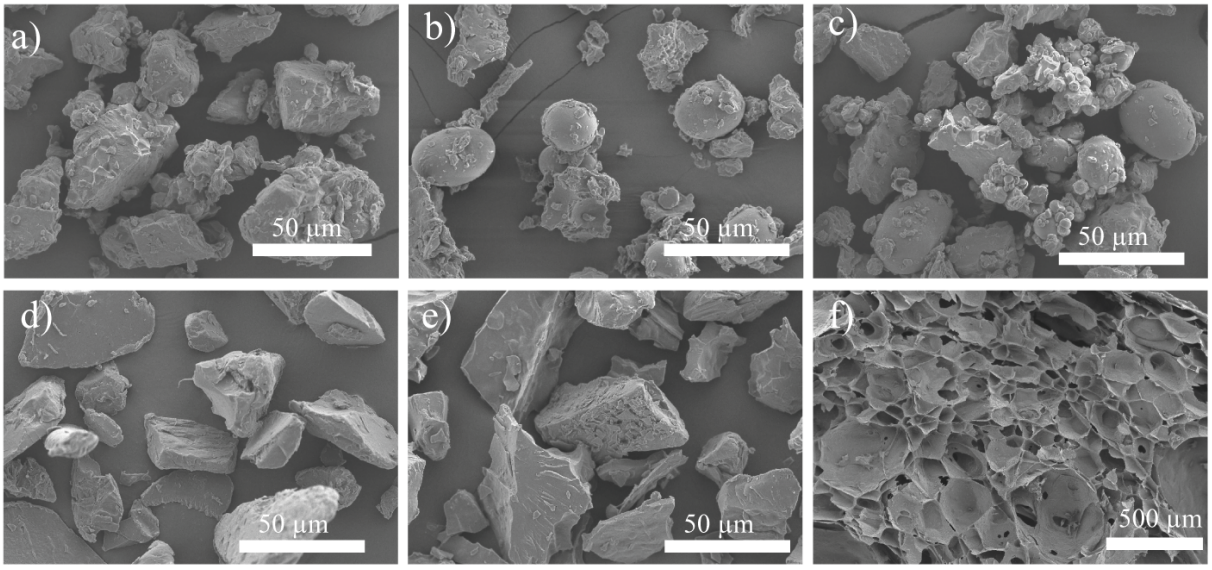

Figure 3. SEM micrographs: (a) white rice, (b) white bean, (c) mixture of raw material and microencapsulated red pitaya, (d) extruded sample, (e) expanded microwave sample.

and an average diameter of approximately 27 μm, indicating a more ordered molecular arrangement and higher crystalline content. Neder-Suárez *et al*. (2023) and Marquezi *et al*. (2016) reported similar results for common and black bean starches. Figure 3c shows the mixture before thermal processing, indicating the combination of rice and white beans as well as encapsulated pitaya. At this stage, native starch granules were still visible because the mixture had not yet undergone gelatinization or structural modification due to heat treatment. The extrusion process modified the structure of starch due to high temperatures, pressures, and shear stress, causing starch gelatinization, partial hydrolysis, and dextrinization, resulting in the loss of its crystalline structure and transition to an amorphous state (Huang *et al*., 2022; Onyango *et al*., 2022; Zambrano *et al*., 2022). As a result, the original granular morphology was disrupted (Figure 3d), resulting in an amorphous irregular surface with a particle size of approximately 28 μm. A structure similar to that of extruded products was observed for the microwave-expanded products (Figure 3e). Similar results were reported by Neder-Suarez *et al*. (2023) for products extruded from corn and beans. During microwave expansion, water inside the pellet becomes steam, generating pressure that expands the product and forms pores of different sizes. This process determines the final texture of the product (Figure 3f); similar results have been reported by Zambrano *et al*. (2024) for 3G extruded snacks enriched with catechin.

Conclusions

In conclusion, SS and ET significantly affected the mechanical, physical, and structural properties of 3G snacks made with rice, beans, and encapsulated red pitaya. The results revealed that high SS and ET increased the values of RTD, DSG, SD, η, G', G", M_f, M_I, and ER but decreased those of ΔE, ΔH, and SME. The extrusion process modified the structure of starch because high temperatures, pressures, and shear stress result in the loss of crystalline structure and transition to an amorphous state. After microwave expansion, similar trends were observed in the responses. A decrease in SS values at similar ETs resulted in the increase in RTD, SME, and ΔH values. Microwave expansion, therefore, reflects a complex interplay between thermal disruption and structural reordering of the starch matrix, resulting in a reduction in SD, DSG, M_f η, and G' and an increase in M_I and G". RTD was negatively correlated with M_f, M_I, η, G', DSG, and SD, suggesting that rapid and efficient processing promotes greater gelatinization of starch. Highest mechanical strength, expansion, and digestibility properties were observed at 125 rpm and 129°C, which promoted more efficient starch transformation. These results are relevant for developing 3G snacks with optimal structural properties and understanding their processing conditions.

Acknowledgements

The authors acknowledge the Universidad Autónoma de Chihuahua (UACH), Universidad Autónoma de Sinaloa (UAS) and Centro de Investigación en

Materiales Avanzados S.C. (CIMAV) for supporting the project. This paper is based on the program "Investigadoras e Investigadores por México, Project number 199", which is supported by Consejo Nacional de Humanidades, Ciencias y Tecnologías (CONAHCYT).

Nomenclature

ET	extrusion temperature
SS	Screw speed
RDT	residence time
SME	specific mechanical energy
DGS	starch gelatinization
SD	*in vitro* digestibility
η	apparent viscosity
G'	storage modulus
G"	loss modulus
ER	expansion ratio
M_f	flexural modulus
M_I	moment of inertia
ΔH	enthalpy
3G	third-generation

References

Acurio, L., Salazar, D., García-Segovia, P., Martínez-Monzó, J. and Igual, M. (2023). Third-generation snacks manufactured from Andean tubers and tuberous root flours: microwave expansion kinetics and characterization. *Foods* 12(11), 2168. https://doi.org/10.3390/foods12112168

Aguilar-Palazuelos, E., Zazueta-Morales, J.D.J., Jiménez-Arévalo, O.A. and Martínez-Bustos, F. (2007). Mechanical and structural properties of expanded extrudates produced from blends of native starches and natural fibers of henequen and coconut. *Starch-Stärke 59*(11), 533-542. https://doi.org/10.1002/star.200700608

Alam, M.S., Kaur, J., Khaira, H. and Gupta, K. (2016). Extrusion and extruded products: changes in quality attributes as affected by extrusion process parameters: a review. *Critical reviews in food science and nutrition 56*(3), 445-473. https://doi.org/10.1080/10408398.2013.779568

Ali, S., Singh, B. and Sharma, S. (2020). Effect of processing temperature on morphology, crystallinity, functional properties, and in vitro digestibility of extruded corn and potato starches. *Journal of Food Processing and Preservation 44*(7), e14531. https://doi.org/10.1111/jfpp.14531

Altan, A., McCarthy, K.L. and Maskan, M. (2009). Effect of extrusion cooking on functional properties and in vitro starch digestibility of barley-based extrudates from fruit and vegetable by-products. *Journal of Food Science 74*(2), E77-E86. https://doi.org/10.1111/j.1750-3841.2009.01051.x

Beltran-Medina, E.A., Jacques-Fajardo, G.E., Berrios, J.J., Suarez-Jacobo, A., Corona-González, R.I., Arriola-Guevara, E. and Guatemala-Morales, G. M. (2025). Assessment on the extrusion parameters, physical and functional properties of a BlueCorn/Red Chief Lentil extrudates added with starch rich amylose and dietary fiber. *Revista Mexicana de Ingeniería Química* 24(2). https://doi.org/10.24275/rmiq/Alim25472

Boukid, F., Klerks, M., Pellegrini, N., Fogliano, V., Sanchez-Siles, L., Roman, S. and Vittadini, E. (2022). Current and emerging trends in cereal snack bars: implications for new product development. *International journal of food sciences and nutrition 73*(5), 610-629. https://doi.org/10.1080/09637486.2022.2042211

Castro-Montoya, Y.A., Jacobo-Valenzuela, N., Delgado-Nieblas, C.I., Ruiz-Armenta, X.A., Heredia, J.B., Delgado-Murillo, S.A., Calderon-Castro A. and Zazueta-Morales, J.J. (2024). Effect of the extrusion process on phytochemical, antioxidant, and cooking properties of gluten-free pasta made from broken rice and nopal. *Revista Mexicana de Ingeniería Química* 23(1). https://doi.org/10.24275/rmiq/Alim24149

Chuang, G.C.C. and Yeh, A.I. (2004). Effect of screw profile on residence time distribution and starch gelatinization of rice flour during single screw extrusion cooking. *Journal of Food Engineering* 63(1), 21-31. https://doi.org/10.1016/S0260-8774(03)00278-4

Cooke, D. and Gidley, M.J. (1992). Loss of crystalline and molecular order during starch gelatinisation: origin of the enthalpic transition. *Carbohydrate research 227*, 103-112. https://doi.org/10.1016/0008-6215(92)85063-6

Delgado-Nieblas, C.I., Ahumada-Aguilar, J.A., Agramón-Velázquez, S., Zazueta-Morales, J.J., Jacobo-Valenzuela, N., Ruiz-Armenta, X.A. and Barraza-Elenes, C. (2021). Physical,

phytochemical and sensory characteristics of extruded high-fiber breakfast cereals prepared by combining carrot by-products with wheat and oat bran. *Revista Mexicana De Ingeniería Química 20*(3), Alim2441-Alim2441. https://doi.org/10.24275/rmiq/Alim2441

García-Cordero, A.L., Jiménez-Alvarado, R., Bautista, M., Díaz-Sánchez, F., Ibarra, I. S., Sánchez-Ortega, I. and Santos, E.M. (2024). Improvement of corn extruded snacks properties by incorporation of pulses Mejora de las propiedades de snacks extrudidos de maíz mediante la incorporación de legumbres. *Revista Mexicana de Ingeniería Química* 23(3). https://doi.org/10.24275/rmiq/Alim24279

Govindaraju, I., Pallen, S., Umashankar, S., Mal, S.S., Kaniyala Melanthota, S., Mahato, D.R. and Mazumder, N. (2020). Microscopic and spectroscopic characterization of rice and corn starch. *Microscopy research and technique 83*(5), 490-498. https://doi.org/10.1002/jemt.23437

Gümüşay, Ö.A. and Şeker, M. (2021). Effects of extrusion parameters on physicochemical properties of third generation corn snacks expanded by microwave heating. *Journal of Food Processing and Preservation 45*(7), e15630. https://doi.org/10.1111/jfpp.15630

Huang, X., Liu, H., Ma, Y., Mai, S. and Li, C. (2022). Effects of extrusion on starch molecular degradation, order–disorder structural transition and digestibility—A review. *Foods 11*(16), 2538. https://doi.org/10.3390/foods11162538

Jan, S., Amin, T., Hussain, S.Z., Jabeen, A., Seh, M.A., Bashir, O. and Wani, S. (2025). Extrusion-aided interaction of rice starch with whey protein isolate: Synergistic influence on physicochemical properties and in vitro starch digestibility characteristics. *Food Chemistry 470*, 142712. https://doi.org/10.1016/j.foodchem.2024.142712

Jia, B., Devkota, L., Sissons, M. and Dhital, S. (2023). Degradation of starch in pasta induced by extrusion below gelatinization temperature. *Food Chemistry 426*, 136524. https://doi.org/10.1016/j.foodchem.2023.136524

Kantrong, H., Charunuch, C., Limsangouan, N. and Pengpinit, W. (2018). Influence of process parameters on physical properties and specific mechanical energy of healthy mushroom-rice snacks and optimization of extrusion process parameters using response surface methodology. *Journal of Food Science and Technology 55*(9), 3462-3472. https://doi.org/10.1007/s13197-018-3271-2

Liu, X., Luan, H., Jinglin, Y., Wang, S., Wang, S. and Copeland, L. (2020). A method for characterizing short-range molecular order in amorphous starch. *Carbohydrate Polymers 242*, 116405. https://doi.org/10.1016/j.carbpol.2020.116405

Liu, X., Zhao, X., Ma, C., Wu, M., Fan, Q., Fu, Y. and Zhang, N. (2024). Effects of extrusion technology on physicochemical properties and microstructure of rice starch added with soy protein isolate and whey protein isolate. *Foods 13*(5), 764. https://doi.org/10.3390/foods13050764

Lu, H., Ma, R., Chang, R. and Tian, Y. (2021). Evaluation of starch retrogradation by infrared spectroscopy. *Food Hydrocolloids 120*, 106975. https://doi.org/10.1016/j.foodhyd.2021.106975

Marquezi, M., Gervin, V.M., Watanabe, L.B., Bassinello, P.Z. and Amante, E.R. (2016). Physical and chemical properties of starch and flour from different common bean (Phaseolus vulgaris L.) cultivars. *Brazilian Journal of Food Technology 19*. https://doi.org/10.1590/1981-6723.0516

Mironeasa, S., Coţovanu, I., Mironeasa, C. and Ungureanu-Iuga, M. (2023). A review of the changes produced by extrusion cooking on the bioactive compounds from vegetal sources. *Antioxidants 12*(7), 1453. https://doi.org/10.3390/antiox12071453

Mohamad, M.M., Talib, R.A., Taip, F.S., Chin, N.L., Sulaiman, R., Shukri, R. and Mohd, N.M.Z. (2020). Changes in the physical properties and specific mechanical energy of corn-mango peel extrudates. *CyTA-Journal of Food 18*(1), 417-426. https://doi.org/10.1080/19476337.2020.1767693

Neder-Suárez, D., Lardizábal-Gutiérrez, D., Meléndez-Pizarro, C.O., Tabio-García, D., Zazueta-Morales, J.D.J., Rodríguez-Roque, M.J. and Quintero-Ramos, A. (2023). Effect in Physical, Thermo-Mechanical Properties, and In Vitro Starch Digestibility of Extruded and Microwave-Expanded Snacks—Mixture of Blue Corn, Black Bean, and Chard:

An Optimization Study. *Starch-Stärke 75*(1-2), 2200158. https://doi.org/10.1002/star.202200158

Neder-Suárez, D., Meléndez-Pizarro, C.O., Pérez-Carrillo, E., Vázquez-Rodríguez, J. A., Valdez-Cárdenas, M. D. C., Ruiz-Gutiérrez, M. G. and Quintero-Ramos, A. (2025). Impact of Vegetal Protein on the Physicochemical and Microstructural Properties of Microencapsulated Mexican Red Pitaya (Stenocereus thurberi) Juice. *AppliedChem 5*(2), 12. https://doi.org/10.3390/appliedchem5020012

Neder-Suárez, D., Quintero-Ramos, A., Meléndez-Pizarro, C.O., de Zazueta-Morales J.J., Paraguay-Delgado, F. and Ruiz-Gutiérrez, M.G. (2021). Evaluation of the physicochemical properties of third-generation snacks made from blue corn, black beans, and sweet chard produced by extrusion. *LTW 146*, 111414. https://doi.org/10.1016/j.lwt.2021.111414

Nwabueze, T.U. and Iwe, M.O. (2010). Residence time distribution (RTD) in a single screw extrusion of African breadfruit mixtures. *Food and Bioprocess Technology 3*(1), 135-145. https://doi.org/10.1007/s11947-008-0056-z

Okunola, A.A., Dottie, E.P., Moses, O.I., Adekanye, T.A., Okonkwo, C.E., Kaveh, M. and Aremu, C.O. (2023). Development and process optimization of a ready-to-eat snack from rice-cowpea composite by a twin extruder. *Processes 11*(7), 2159. https://doi.org/10.3390/pr11072159

Onyango, C. and Mutungi, C. (2008). Synthesis and in vitro digestion of resistant starch type III from enzymatically hydrolysed cassava starch. *International Journal of Food Science and Technology 43*(10), 1860-1865. https://doi.org/10.1111/j.1365-2621.2008.01764.x

Oyeyinka, S.A. Akintayo, O.A., Adebo, O.A., Kayitesi, E., and Njobeh, P.B. (2021). A review on the physicochemical properties of starches modified by microwave alone and in combination with other methods. *International Journal of Biological Macromolecules 176*, 87-95. https://doi.org/10.1016/j.ijbiomac.2021.02.066

Panak Balentić, J., Babić, J., Jozinović, A., Ačkar, D., Miličević, B., Muhamedbegović, B. and Šubarić, D. (2018). Production of third-generation snacks. *Croatian journal of food science and technology 10*(1), 98-105. https://doi.org/10.17508/CJFST.2018.10.1.04

Pensamiento-Niño, C.A., Gómez-Aldapa, C.A., Hernández-Santos, B., Juárez-Barrientos, J.M., Herman-Lara, E., Martínez-Sánchez, C.E. and Rodríguez-Miranda, J. (2018). Optimization and characterization of an extruded snack based on taro flour (Colocasia esculenta L.) enriched with mango pulp (Mangifera indica L.). *Journal of Food Science and Technology 55*(10), 4244-4255. https://doi.org/10.1007/s13197-018-3363-z

Qiu, C., Hu, H., Chen, B., Lin, Q., Ji, H. and Jin, Z. (2024). Research Progress on the Physicochemical Properties of Starch-Based Foods by Extrusion Processing. *Foods 13*(22), 3677. https://doi.org/10.3390/foods13223677

Ruiz-Gutiérrez, M.G., Amaya-Guerra, C.A., Quintero-Ramos, A., Pérez-Carrillo, E., Ruiz-Anchondo, T.D.J., Báez-González, J.G. and Meléndez-Pizarro, C.O. (2015). Effect of extrusion cooking on bioactive compounds in encapsulated red cactus pear powder. *Molecules*, *20*(5), 8875-8892. https://doi.org/10.3390/molecules20058875

Serna-Saldivar, S.O. (Ed.). (2022). *Snack Foods: Processing, Innovation, and Nutritional Aspects*. CRC Press.

Singha, P., Muthukumarappan, K. and Krishnan, P. (2018). Influence of processing conditions on apparent viscosity and system parameters during extrusion of distiller's dried grains-based snacks. *Food Science and Nutrition 6*(1), 101-110. https://doi.org/10.1002/fsn3.534

Temgire, S., Borah, A., Kumthekar, S. and Idate, A. (2021). Recent trends in ready to eat/cook food products. *Pharma Innov. J*, *10*(5), 211-217.

Tyl, C., Bresciani, A., and Marti, A. (2021). Recent progress on improving the quality of bran-enriched extruded snacks. *Foods* 10(9), 2024. https://doi.org/10.3390/foods10092024

Van der Sman, R.G.M. and Bows, J.R. (2017). Critical factors in microwave expansion of starchy snacks. *Journal of Food Engineering 211*, 69-84. https://doi.org/10.1016/j.jfoodeng.2017.05.001

Wang, N., Li, C., Miao, D., Dai, Y., Zhang, H., Zhang, Y. and Wang, B. (2023). Effect of improved extrusion cooking technology (IECT) on structure, physical properties and in vitro digestibility of starch. *International Journal of Biological Macromolecules 252*, 126436. https://doi.org/10.1016/j.ijbiomac.2023.126436

Wu, Q., Zhang, X., Gao, F. and Wu, M. (2023). Study on the residence time and texture prediction of pea protein extrusion based on image analysis. *Foods 12*(24), 4408. https://doi.org/10.3390/foods12244408

Wu, W., Jiao, A., Xu, E., Chen, Y. and Jin, Z. (2020). Effects of extrusion technology combined with enzymatic hydrolysis on the structural and physicochemical properties of porous corn starch. *Food and Bioprocess Technology 13*(3), 442-451. https://doi.org/10.1007/s11947-020-02404-1

Yao, T., Ma, M. and Sui, Z. (2023). Structure and function of polysaccharides and oligosaccharides in foods. *Foods*, *12*(20), 3872. https://doi.org/10.3390/foods12203872

Zambrano, Y., Contardo, I., Moreno, M.C. and Bouchon, P. (2022). Effect of extrusion temperature and feed moisture content on the microstructural properties of rice-flour pellets and their impact on the expanded product. *Foods 11*(2), 198. https://doi.org/10.3390/foods11020198

Zambrano, Y., Mariotti-Celis, M.S. and Bouchon, P. (2024). 3G extruded snacks enriched with catechin for high antioxidant capacity. *LWT 192*, 115674. https://doi.org/10.1016/j.lwt.2023.115674

Zhang, C., Xue, W., Li, T. and Wang, L. (2023). Understanding the relationship between the molecular structure and physicochemical properties of soft rice starch. *Foods 12*(19), 3611. https://doi.org/10.3390/foods12193611